Planta (2009) 230:795–805
DOI 10.1007/s00425-009-0985-4

ORIGINAL ARTICLE

LeFRK2 is required for phloem and xylem differentiation and the transport of both sugar and water

Hila Damari-Weissler · Shimon Rachamilevitch · Roni Aloni · Marcelo A. German · Shabtai Cohen · Maciej A. Zwieniecki · N. Michele Holbrook · David Granot

Received: 14 May 2009 / Accepted: 7 July 2009 / Published online: 25 July 2009

Abstract It has been suggested that *LeFRK2*, the major fructose-phosphorylating enzyme in tomato plants, may be required for stem xylem development. Yet, we do not know if this enzyme affects the development of individual vessels, whether it affects water conductance, or whether it affects phloem development and sugar transport. Here, we show that suppression of *LeFRK2* results in a significant reduction in the size of vascular cells and slows fiber maturation. The vessels in stems of *LeFRK2*-antisense plants are narrower than in WT plants and have thinner secondary cell walls. Although the cambium produces rounded secondary vessels, these vessels become deformed during the early stages of xylem maturation. Water conductance is then reduced in stems, roots, and leaves, suggesting that *LeFRK2* influences xylem development throughout the entire vascular system. Interestingly, the build-up of positive xylem pressure under static (no-flow) conditions was also decreased. Suppression of *LeFRK2* reduced the length and width of the sieve elements, as well as callose deposition. To examine the effect of *LeFRK2* suppression on phloem transport, we created triple-grafted plants in which a portion of the wild-type stem was replaced with an antisense interstcok, and compared the contents of the transported sugar, sucrose, in the different portions of these stems. Sucrose contents above and within the *LeFRK2*-antisense interstock were significantly higher than those below the graft. These results show that the antisense interstock restricted the downward movement of sucrose, suggesting that *LeFRK2* is required for both phloem and xylem development.

Keywords Antisense · Fructokinase · Fructose · Phloem · Sucrose · Xylem

Abbreviations

FRK	Fructokinase
HXK	Hexokinase
SuSy	Sucrose synthase
VPD	Vapor pressure deficit

Introduction

Sucrose is an important end product of photosynthesis and the main sugar transported in the vascular systems of many

Contribution No. 114/2009 from the Volcani Center ARO.

H. Damari-Weissler · M. A. German · D. Granot (✉)
Institute of Plant Sciences,
Agricultural Research Organization,
The Volcani Center, Bet Dagan 50250, Israel
e-mail: granot@agri.gov.il

S. Rachamilevitch
Albert Katz Department of Dryland Biotechnologies,
Blaustein Institute for Desert Research, Ben Gurion University,
Sede Boqer Campus, Midreshet Ben-Gurion 84990, Israel

R. Aloni
Department of Plant Sciences,
Tel Aviv University, Tel Aviv 69978, Israel

S. Cohen
Institute of Soils, Water and Environmental Sciences,
Agricultural Research Organization,
The Volcani Center, Bet Dagan 50250, Israel

M. A. Zwieniecki
Arnold Arboretum, Harvard University,
16 Divinity Ave., Cambridge, MA 02138, USA

N. Michele Holbrook
Organismic and Evolutionary Biology, Harvard University,
16 Divinity Ave., Cambridge, MA 02138, USA

plants, including tomato. Some of the transported sucrose is cleaved in the vascular tissues to support vascular development and functioning. Sucrose, a disaccharide, must be cleaved by either sucrose synthase (SuSy), likely the main sucrose cleaving enzyme in the vascular system, into UDP-glucose and fructose, or by invertase into glucose and fructose (Koch 2004). Consequently, fructose is destined to be the main monosaccharide produced through the cleavage of sucrose. Free fructose must first be phosphorylated by either hexokinase (HXK) or fructokinase (FRK) for further metabolism, otherwise, the accumulating fructose might feedback inhibit SuSy activity, reducing sucrose cleavage (Schaffer and Petreikov 1997). HXK and FRK are distinguished by their substrate specificities and affinities (Renz and Stitt 1993; Dai et al. 2002b; Granot 2007). HXK may phosphorylate both glucose and fructose, but its affinity to fructose is two orders of magnitude lower than its affinity to glucose, as well as two orders of magnitude lower than the affinity of FRK to fructose. It is, therefore, likely that fructose is primarily phosphorylated by FRK (Granot 2007).

Four different FRK-encoding genes, denoted *LeFRK1-4*, have been isolated from tomato (*Solanum lycopersicon*) plants (Kanayama et al. 1997, 1998; German et al. 2002, 2004; Granot 2007). *LeFRK2* is the major FRK gene expressed in most tissues, including stems, roots, and leaves (Kanayama et al. 1997, 1998; German et al. 2002, 2004). To study the role of *LeFRK2* in tomato plants, we previously generated and analyzed transgenic tomato plants with antisense suppression of *LeFRK2* (Dai et al. 2002a; German et al. 2003) or co-suppression. These antisense plants exhibited growth inhibition and wilting of young leaves during the day. Triple-grafting experiments, in which an antisense interstock replaced a portion of the wild-type stem, demonstrated that an antisense interstock is sufficient to inhibit growth and cause leaf wilting, suggesting that *LeFRK2* is required for proper stem functioning. Furthermore, the cumulative area of active xylem in stems of antisense plants was smaller than that of wild-type plants, suggesting that *LeFRK2* is required for stem xylem development. Accordingly, it has been postulated that suppression of *LeFRK2* might affect water transport in tomato stems (German et al. 2003). However, the specific effects of *LeFRK2* suppression on stem xylem development and water conductance have not been examined. Furthermore, *LeFRK2* is expressed not only in stems, but also in roots and leaves (German et al. 2004) with the effects of its suppression on roots and leaves being unknown. The effect of *LeFRK2* suppression on phloem structure and transport is also unknown. In this study, we analyzed the effects of *LeFRK2* suppression on vessel and sieve-tube development, water conductance in stems, leaves and roots and sugar transport in the phloem.

Materials and methods

Plant material

LeFRK2-antisense plants are the transgenic tomato (*Solanum lycopersicon* cv MP1) plants with antisense suppression of *LeFRK2*, previously described in (Dai et al. 2002a; German et al. 2003).

Anatomical techniques

For analyzing the longitudinal structure of both the sieve tubes and vessels, the stem tissues were cut and transferred to 70% ethanol for two days. The stem tissue was then transferred to 90% lactic acid, where it was cleared by boiling for 1 min. The tissues were kept in lactic acid at room temperature for a few days and the phloem was separated from the xylem in the cambium zone under a dissecting stereoscope. Longitudinal sections were prepared from the xylem, while the whole cleared phloem (including all the tissues from the cambium to the epidermis) was analyzed without any sectioning. The tissues were stained with a 0.4% lacmoid solution (Polyscience, Warrington, Pa, USA) in 90% lactic acid for 2 h and then rinsed in tap water until the color of the tissues changed from red to blue within about 1 h (Aloni 1980). The change in color indicates a very important step in this procedure, a pH change from acid to alkaline. Lacmoid stains lignin, hence vessels and fibers appear marine blue and callose depositions on the sieve plates are dyed a turquoise blue. For microscopic analysis, the stained tissues were transferred to 50% sodium lactate and were then observed under transmitted white light. The cleared phloem was observed from the cambium side.

In addition, both the phloem and the xylem tissues were also studied in free-hand cross-sections taken from the center of various internodes along the stems of both the *LeFRK2*-antisense and the wild-type plants. The cross-sections were stained for a few seconds in 2% lacmoid in 96% ethanol, then rinsed in tap water for a few minutes, mounted in 50% sodium lactate (Aloni 1980) and observed under transmitted white light.

Measurements of stomata size and density

For the measurements of stomatal morphology and density, epidermal impressions were made of intact young leaves of four-week-old plants. A solution of 4% Formvar resin (Ted Pelle Inc., Redding, CA, USA) in 1,2 dichloroethane was applied to the lower surface of Leaf no. 7. After drying (1 to 3 min), the imprints were removed from the leaf with clear adhesive tape and glued onto a microscope slide. All samples were taken interveinally, in the center of the longitudinal

axis of the leaf, halfway between the midrib and the margins. Stomatal aperture and density were analyzed from digital images of the epidermal imprints captured with a digital camera.

Measurements of whole plant transpiration in response to VPD

Plants were grown in a glasshouse in 5-l pots until they had developed 12–14 fully expanded leaves. The transpiration rate response to vapor pressure deficits (VPD) was measured in the laboratory by installing the plant shoot in a chamber for regulation of VPD (Sinclair et al. 2008). A box fan was placed inside the shoot chamber to rapidly stir the air and minimize boundary layer conductance and its impact on plant water loss rate. Absolute humidity in the shoot chamber was adjusted by changing the rate of airflow (15–45 l min^{-1}) through the shoot chamber and the humidity of the air. The plant shoot was exposed to 800 μmol m^{-2} s^{-1} photosynthetically active radiation and maintained at a temperature of 26 ± 1°C. Air temperature and leaf temperature were measured and rarely differed by more than 0.3°C. Air VPD was calculated based on the measured air temperature and the relative humidity in the chamber. A balance was placed under the pot to measure changes in plant weight. As the plant stem was not sealed in the shoot chamber, the stem could move freely in a slot of the chamber and not interfere with the measurement of plant weight. Weight was recorded every 30 s. Once a new level of humidity was established in the chamber, a new steady transpiration rate was usually reached in about 20 min. Transpiration rate was calculated by linear regression during the steady-state period from the decrease in pot weight over 20 min. Data were collected from at least five plants for each genotype. Transpiration rates for individual plants and treatments were plotted against the VPD to which the plant shoots were exposed.

Hydroponic treatment

Seeds were planted on wet filter paper (Whatman Quantitative Circles, 90 mm, Cat. No. 1001 090, Whatman®, Schleicher & Schuell, Dassel, Germany) in covered Petri dishes and left to germinate in darkness at room temperature. Three days after germination, the seedlings were moved to aerated hydroponic culture in 6.5-l containers filled with modified Hoagland solution (pH ~ 6.1; 795 μM KNO_3, 603 μM $Ca(NO_3)_2$, 270 μM $MgSO_4$, and 109 μM KH_2PO_4; micronutrients: 40.5 μM Fe(III)-EDTA, 20 μM H_3BO_4, 2 μM $MnSO_4$, 0.085 μM $ZnSO_4$, 0.15 μM $CuSO_4$, and 0.25 μM Na_2MoO_4) and maintained in a growth chamber (PAR 600 mM, temperature 25°C day and 21°C night, humidity 65%). After 1 week, the young plants were transferred to 42-l boxes (12 plants per box) and the culture media was replaced two times per week.

Forced root exudation

The hydraulic conductance of tomato root systems was determined by measuring the flow induced in response to an applied pressure gradient (Gorska et al. 2008). Detopped root systems were fitted with a plastic tube filled with DI water and connected to a beaker located on a balance (±0.01 mg). The root system was sealed in a chamber containing the hydroponic solution in which the plants had been grown. The pH was kept at ~6.1 using MES (2-(*N*-morpholino) ethanesulfonic acid) buffer (1 g per l). The pressure in the chamber was regulated using a needle valve, which was adjusted so as to allow a small leak in the chamber, such that air used to pressurize the chamber also served to aerate the medium. Water flow through the root system was automatically recorded by a computer at 30 s intervals. Flow stabilization occurred 10–20 min after the plant was exposed to pressure. Flow data were then collected for a 60-min period. At the end of each experiment, the fresh weights of roots and shoots were recorded. The stems and roots were then dried in an oven for 72 h at 90°C, after which the dry weights of these tissues were recorded and the root: shoot ratio was calculated (Gorska et al. 2008).

Preparation of roots for scanning and image analysis

Root parameters were assessed as described in German et al. (2000) with some modifications. Excised roots of 4-week-old plants (wild-type and antisense) were stained in 10 g/l methylene blue solution for 5 min, rinsed twice by immersion in tap water for 2 min, and placed on a glass-bottom tray. Root branches were separated from each other and covered with a transparent net to hold them in place. Contrast was achieved by placing a white cover above the net. Roots were scanned with a Delta-T Scan (Delta-T Devices, Burwell, UK). Root images were converted to black and white figures using HP DeskScan II software (Hewlett-Packard, USA) and saved as tif files using Corel Photo-Paint software (Corel, Ontario, Canada). The image analysis was performed using Delta-T Scan software (Delta-T Devices).

Stem hydraulic conductivity

Stem hydraulic conductivity (K_h) was assessed on 5–10 main stems of each genotype using stem pieces 5–10 cm in length; a preliminary assessment showed that segment length did not affect K_h, as long as each segment was at least 5 cm long. Deionized, degassed, and filtered (0.2 μm filters) water was used as a perfusion solution. Stems were

first perfused under elevated pressure (150 kPa) to remove any embolisms, then hydraulic conductivity was calculated as the pressure difference across the stem divided by the volumetric flow and stem length. Xylem cross-sectional area was microscopically determined for each stem to allow the calculation of the xylem-specific conductivity (K_s, which equals K_h divided by total xylem area). The cross-sectional vessel lumen area was also microscopically determined for each stem so that lumen-specific conductivity (K_{ls}; K_h divided by total vessel lumen area) could be determined. Leaf area distal to each measured stem was determined with an area meter (LI-3100; Li-Cor, Lincoln, Neb., USA), allowing for leaf specific conductivity (K_L; K_h divided by leaf area) to be determined (Kocacinar and Sage 2004).

Leaf hydraulics as measured by rehydration

Whole stems were detached from greenhouse-grown plants and allowed to dry briefly on a laboratory bench to a leaf water potential of −0.3 to −0.7 MPa. After this brief drying, a stem segment associated with a single leaf was placed in a guillotine-like apparatus that allowed the petiole to be severed from the stem segment under water and the cut petiole to be connected to a water reservoir in a single step (Zwieniecki et al. 2007). The water reservoir was placed on a high-resolution balance (±10 μg) and the amount of water taken up by the rehydrating leaf was recorded every 1 s. Rehydration was performed while the submerged leaf was exposed to approximately 800 μmol m^{-2} s^{-1} photosynthetically active radiation. Preliminary measurements showed that submerging the lamina did not alter leaf water potential, indicating that water uptake through the leaf surface did not influence the measurement. Water uptake kinetics were analyzed assuming a two-compartment, exponential model (Zwieniecki et al. 2007). Time constants for rehydration and hydraulic conductance were calculated for the fast-uptake compartment, which was assumed to be indicative of water flow in the epidermal compartment of the leaves. A total of eight plants, one leaf per plant, of each genotype were measured.

Sugar assays

Sugars were extracted from stem segments by resuspending the segments in 5 ml of 80% ethanol in an 80°C water bath for 60 min. This procedure was repeated twice. The ethanol solutions were combined and completely evaporated at 40°C with the aid of continuous ventilation. The dried sugars were dissolved in 1 ml distilled water and were stored frozen (−80°C) until they could be analyzed. Sucrose, fructose, and glucose contents were determined by HPLC. The HPLC system consisted of a Shimadzu LC10AT solvent delivery system and detection was by a Shimadzu RID10A refractive index detector. Separation was carried out on an Alltech 700 CH Carbohydrate Column (Alltech, Deer-field, IL, USA), maintained at 90°C with a flow rate of 0.5 ml/min, according to manufacturer's recommendations.

The ethanol-insoluble residue was used to determine the concentration of starch in the grafted segment of the stem. Starch digestion was carried out by incubating and autoclaving samples with 6 ml water, and then adding 4 ml of buffer containing 200 units of amyloglucosidase and incubating overnight at 55°C (Dinar et al. 1983). The amount of released glucose was determined using Sumner reagent. Optical density was determined at 550 nm.

Results

Reduced xylem cell size, slow fiber differentiation, and deformation of secondary vessels

Suppression of *LeFRK2* substantially reduces the size of xylem cells (Fig. 1a–c), in comparison to those of wild-type tomato plants (Fig. 1d–f). The secondary xylem of *LeFRK2* antisense stems has an anatomical phenotype characterized by deformed, narrow secondary vessels (Figs. 1a, b, 2b). The narrow cambium in the *LeFRK2*-antisense stems indicates that there is a low level of meristematic activity in the cambium (Fig. 1a), as compared with the active cambium of wild-type stems (Fig. 1d). Tomato stems produce secondary xylem fibers (also known as libriform fibers), which are cambial derivatives, but do not produce fibers in the primary xylem (Fig. 2b). In *LeFRK2*-antisense stems, the secondary fibers differentiate slowly and therefore form near the cambium, a region of growing fibers, with thin secondary cell walls and dense cytoplasm (stained dark blue and marked by a white F in Fig. 1a). These slowly expanding fibers likely apply pressure on the differentiating secondary vessels, which have thin secondary cell walls, resulting in various patterns of deformed vessels (Figs. 1a,b, 2b). Near the cambium, the secondary vessels of the antisense stems start off as round vessels, and then become increasingly deformed (Fig. 1a) with increasing distance from the cambium. In contrast, the narrow primary vessels of the antisense plants, which are surrounded by parenchyma cells, remain round (Fig. 2b). In wild-type stems, the secondary fibers differentiate rapidly and produce thick secondary cell walls, which do not expand and do not affect the thick secondary cell walls of the vessels (Fig. 1d,e).

A second major difference in xylem development was observed in axial patterns of vessel differentiation. It is well known that, along the plant axis, the vessels become gradually wider with increasing distance from the young leaves (Aloni and Zimmermann 1983). Near the roots, at the base

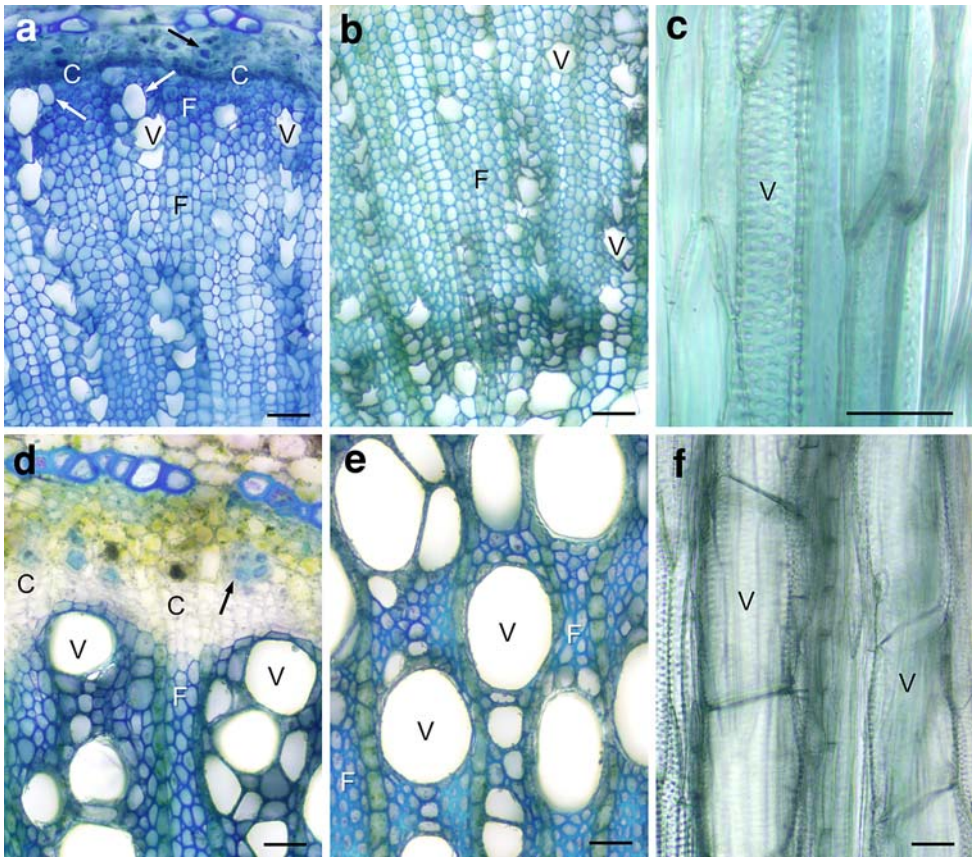

Fig. 1 Xylem and phloem structure in *LeFRK2*-antisense (**a**–**c**) and wild-type (**d**–**f**) tomato stems. **a** Cross-section from the middle of a stem showing that suppression of *LeFRK2* reduces cambium (C), vessel (V), and sieve-element (*black arrow*) width, and slows fiber differentiation, resulting in a few layers of differentiating fibers (*white F*) with dense cytoplasm. Note that the secondary vessels near the cambium differentiate with a circular shape (*white arrows*) and become deformed (V) away from the cambium. Mature fibers (*black F*) are narrow and have thin cell walls. **b** Xylem from the base of the stem characterized by deformed vessels and narrow fibers (F) both with thin cell walls. **c** Longitudinal section from stem base showing a vessel surrounded by secondary xylem fibers. **d** Cross-section from the middle of a wild-type stem characterized by wide cambium, large vessels, and sieve tubes (*arrow*), and mature fibers (F). **e** Widest vessels and fibers, both with thick secondary walls, from a stem base. **f** Longitudinal section from a stem base showing two wide vessels. *Scale bars* = 50 μm

of the wild-type stems, the late-formed vessels were the widest (Fig. 1e), while there was no significant increase in vessel width at the base of the *LeFRK2*-antisense stems (Fig. 1b).

Suppression of *LeFRK2* results in short, narrow sieve elements

Likewise, the suppression of *LeFRK2* substantially reduced the size of sieve elements in both the external phloem (Figs. 1a, 2a) and the internal phloem (Fig. 2b, c) to less than half of the normal size of sieve elements in the external phloem (Figs. 1d, 2d) and internal phloem (Fig. 2e, f) of the wild-type stems. In addition, the sieve elements of the *LeFRK2*-antisense stems had less callose on their sieve plates (Fig. 2a) than the wild-type sieve elements (Fig. 2d). Interestingly, there was no fiber differentiation in the internal phloem (Fig. 2b, c) of the *LeFRK2*-antisense stems; whereas the internal phloem of the wild-type stems was characterized by the formation of primary phloem fibers (Fig. 2e, f).

Whole plant transpiration is reduced

To determine the effect of *LeFRK2* suppression on water use, we followed the transpiration rate of whole plants at different VPD and compared these rates with that of wild-type plants. *LeFRK2*-antisense plants had significantly lower transpiration rates at all VPD levels (Fig. 3). Even under very humid conditions (low VPD), the transpiration rate of *LeFRK2*-antisense plants was lower than that of the wild-type plants. The response to increasing VPD for both types of plants could be described as two linear regressions, indicating a higher stomatal conductance at low VPD and then a transition point at which stomatal apertures were reduced. The slopes of both regression lines and the VPD at which stomata closed were lower for the *LeFRK2*-antisense plants. Lower transpiration rates could not be attributed to

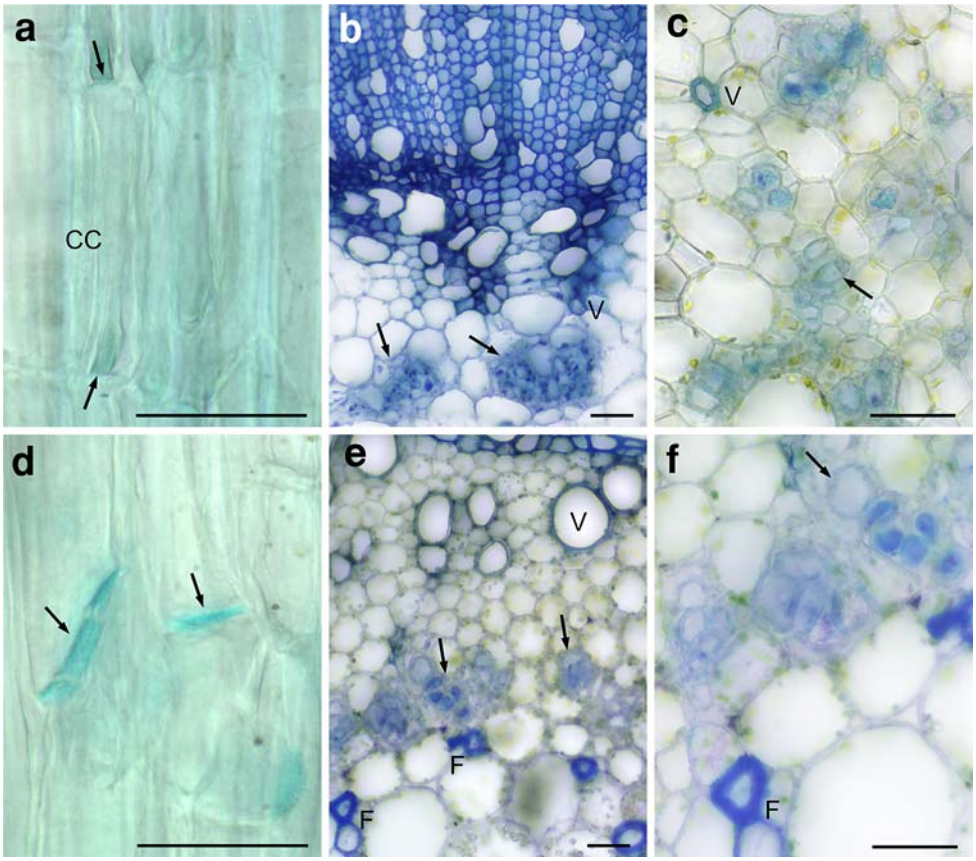

Fig. 2 Phloem and xylem structure in *LeFRK2*-antisense (**a**–**c**) and wild-type (**d**–**f**) tomato stems. **a** Longitudinal section from the base of the antisense stem showing short and narrow sieve elements with almost no callose on the sieve plates (*arrows*) and a companion cell (CC). **b** Cross-section from the middle of antisense stems showing internal phloem (*arrows*) and narrow ring-patterned primary vessels (V). **c** Internal phloem with narrow sieve elements (*arrow*) and a primary vessel (V). **d** Longitudinal section from the base of a wild-type stem showing wide sieve elements with callose deposits on their sieve plates (*arrows*). **e** Cross-section from the middle of a wild-type stem showing internal phloem (*arrows*) with primary phloem fibers (F) and wide primary vessels (V). **f** Internal phloem with wide sieve elements (*arrow*) and fibers (F). *Scale bars* = 50 μm

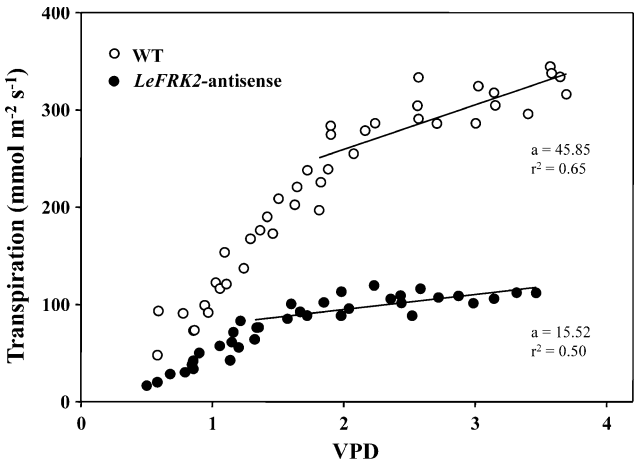

Fig. 3 Whole plant transpiration in response to VPD. Transpiration rate plotted against atmospheric VPD for each observation of each of the two genotypes. The transpiration rates were calculated on a leaf area basis for each individual plant ($n = 5$). The numbers on the graph are the slopes (mg H_2O m^{-2} leaf area s^{-1} kPa^{-1}) obtained from linear regressions for the segments where VPD was linear above 1.5 kPa

differences in stomatal structure as the number and size of the stomata were similar in wild-type and antisense plants (Table 1). These results support our previous suggestion that the wilting of *LeFRK2*-antisense plants could not be attributed to increased water loss through the leaves, but rather to reduced water uptake or transport.

Table 1 Mean values for stomatal size and density of wild-type and *LeFRK2*-antisense leaves

	Wild-type	*LeFRK2*-antisense
Guard cell aperture (μm^2)	0.26 ± 0.01	0.21 ± 0.04
Guard cell density (mm^{-2})	146.9 ± 8.6	160.6 ± 11.4

Results represent five replications for all parameters

Suppression of *LeFRK2* leads to reduced water conductance in the stem

The measured hydraulic capacity of young *LeFRK2*-antisense stems was significantly less than that of wild type stems (Table 2). The hydraulic conductance per length (K_h) was significantly (79%) less in the antisense plants, reflecting both the altered xylem anatomy and the smaller stem diameter of the plants lacking FRK2 activity. When normalized to xylem cross-sectional area (K_s), the hydraulic conductivity of the antisense plants was 67% lower than in WT plants. When hydraulic conductivity was calculated relative to the summed lumen area of xylem vessels (K_{ls}) the reduction was 58%, reflecting the preponderance of smaller diameter conduits in the antisense plants. Finally, leaf specific hydraulic conductivity (K_L) was reduced by 59% relative to WT, consistent with their propensity to wilt.

Table 2 Stem water conductance in wild –type and *LeFRK2*-antisense plants

	Wild-type	*LeFRK2*-antisense
K_h (kg s^{-1} m MPa^{-1}) × 10^{-5}	1.46 ± 0.13[a]	0.31 ± 0.04[b]
K_s (kg s^{-1} m^{-1} MPa^{-1})	2.13 ± 0.25[a]	1.43 ± 0.17[b]
K_{ls} (kg s^{-1} m^{-1} MPa^{-1})	36.46 ± 4.26[a]	21.11 ± 2.31[b]
K_L(kg s^{-1} m^{-1} MPa^{-1}) × 10^{-4}	5.79 ± 0.64[a]	3.42 ± 0.23[b]

Stem hydraulic conductivity (K_h), xylem-specific conductivity (K_s), lumen specific conductivity (K_{ls}) and leaf specific conductivity (K_L) were determined for eight wild-type and eight *LeFRK2*-antisense plants. Means (±SE) of eight plants. Different letters represent values that are significantly different (Student's *t* test; $P < 0.05$) between wild-type and antisense plants

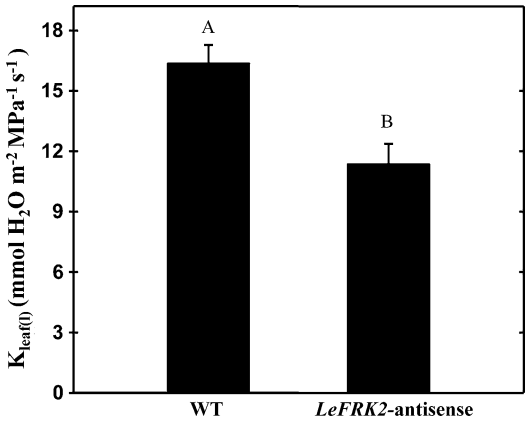

Fig. 4 Leaf water conductance in wild-type and *LeFRK2*-antisense plants. Leaf hydraulic properties were measured by leaf rehydration. Data are the means ± SE of eight plants. Different letters represent values that are significantly different (student's *t* test; $P < 0.05$)

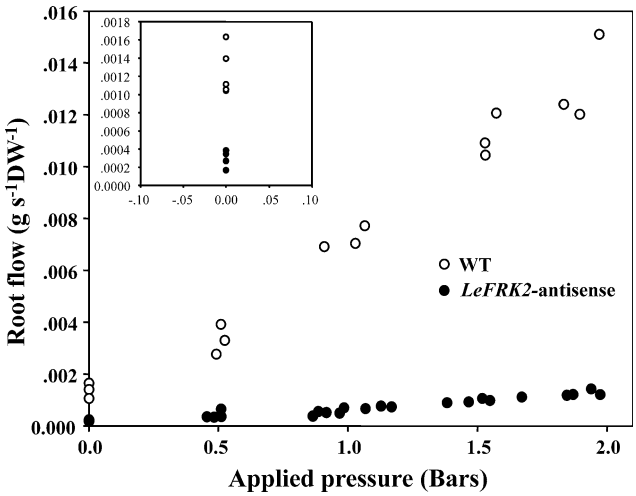

Fig. 5 Root water flow in *LeFRK2*-antisense plants. Pressure-driven exudation from whole root systems of the two genotypes. Circular points are average values of six plants. *Inset figure* depicts root pressure when no external pressure was applied

Effects on leaf and root water conductance

LeFRK2 is expressed not only in stems, but also in leaves and roots (German et al. 2004), therefore suppression of *LeFRK2* might affect water transport in leaves and roots independent of its effect on stem hydraulic conductivity. Leaf hydraulic conductance (mmol H_2O m^{-2} MPa^{-1} s^{-1}) in the antisense plants was 30% less than in the wild-type plants (Fig. 4). Root conductivity was also significantly reduced (Fig. 5). Surprisingly, unlike wild-type plants, roots of *LeFRK2*-antisense plants exhibited almost zero root pressure (Fig. 5). Under anoxic conditions, root hydraulic conductivity of wild-type and *LeFRK2*-antisense plants was reduced by a similar percentage (not shown), implying that the reduced conductivity of *LeFRK2*-antisense plants could not be attributed to any effect of *LeFRK2* on aquaporins (Gorska et al. 2008).

Effect on sugar transport

Narrow and short sieve elements (Fig. 2) are expected to reduce sucrose transport, similar to the reduced transport through narrow and short sieve elements of phloem anastomoses (Aloni and Peterson 1990). We used a functional approach to study the effect of antisense suppression of *LeFRK2* on phloem transport. Specifically, we created triple-grafted plants in which *LeFRK2*-antisense interstock replaced a portion of the stem of wild-type plants (Fig. 6) and measured the amount of sugar in each part of the triple graft, above, within, and below the interstock. We assumed that if suppression of *LeFRK2* affected phloem transport in the *LeFRK2*-antisense interstock, sucrose might accumulate in the stem above and within the interstock. Indeed, the amounts of sucrose above and within the *LeFRK2*-antisense interstock were significantly greater than the amounts below the graft (Fig. 7a), while sucrose levels in control triple grafts (with a wild-type interstock) were similar above, within, and below the interstock. These results suggest that suppression of *LeFRK2* restricts sucrose transport in the stem of *LeFRK2*-antisense plants, likely due to their narrow, short sieve elements. Unlike control plants, fructose and glucose levels were also higher mainly within and above the *LeFRK2*-antisense interstcok (Fig. 7b), indicating lower rate of sugar metabolism. Yet, starch was found at similar levels in the different portions of the triple grafts in both the control and antisense treatments (Fig. 7c).

LeFRK2 suppression affects upward water transport independent of phloem transport

The restriction on downward sugar transport could potentially affect root development, which might in turn affect

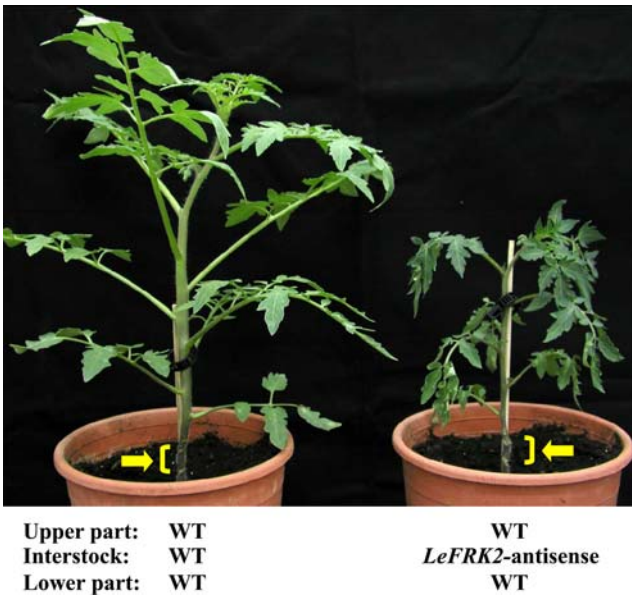

Fig. 6 Triple-grafting of *LeFRK2*-antisense and wild-type plants. Graftings were performed in two consecutive steps (10 days apart) at the seedling stage. These plants were photographed about 4 weeks after the second grafting. The *yellow arrows* and *brackets* indicate the location of the grafts

water uptake. Indeed, roots of *LeFRK2*-antisense plants were smaller than those of wild-type plants (Table 3). Yet, the root:shoot ratio of *LeFRK2*-antisense plants increased (Fig. 8), indicating that roots were less affected than shoots. Nevertheless, the growth inhibition and leaf wilting observed in *LeFRK2*-antisense plants could still be the result of inhibited root water uptake, which could be due to reduced transport of sugar to the roots. To discriminate between the effects of reduced upward water transport and reduced downward sugar transport on growth inhibition and leaf wilting, we grafted a stem segment of *LeFRK2*-antisense plants onto wild-type plants in such a way that a wild-type bud could emerge from the lower wild-type scion onto which the antisense segment was grafted (Fig. 9). The wild-type lateral buds emerging from the lower wild-type scion developed normally and supported the normal development of the root system (not shown). Nevertheless, the central wild-type shoot grafted onto the antisense interstock was stunted (Fig. 9, rightmost shoot in right panel) and wilted during the day, resembling the phenotype of the *LeFRK2*-antisense plants. These grafting experiments demonstrate that the antisense-like phenotype of the wild-type shoot imposed by the antisense interstock occurred independently of root development and function, suggesting that water transport through the xylem was the primary cause of growth inhibition and the observed wilting.

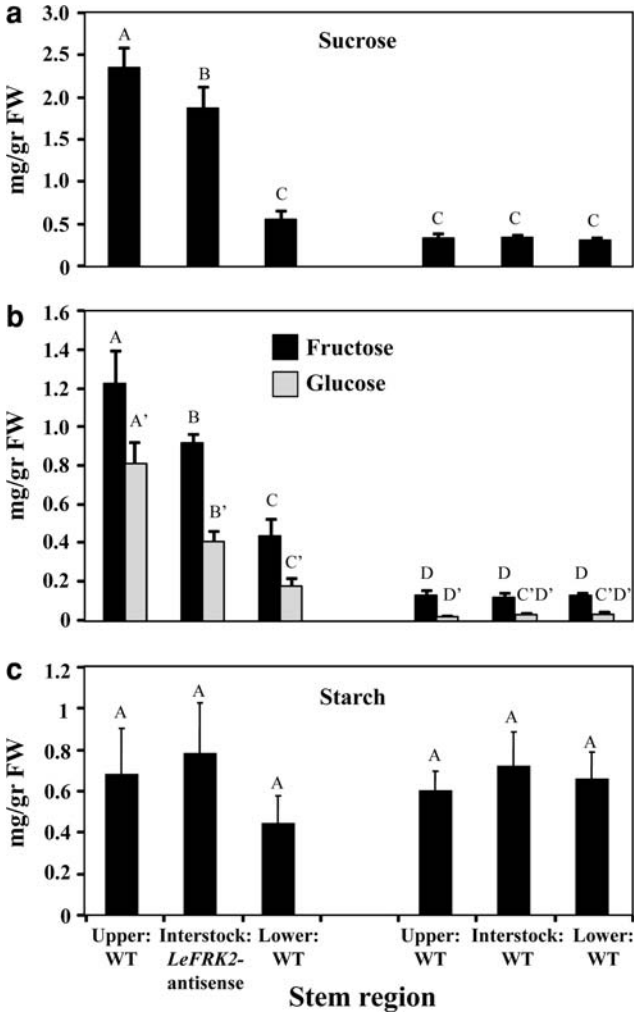

Fig. 7 Sucrose, fructose, glucose, and starch content in stem portions of the triple-grafted plants. Data are the means ± SE of eight plants. Statistical analysis has been done for each sugar independently. *Different letters* represent values that are significantly different (student's *t* test; $P < 0.05$)

Table 3 Root parameters in 4-week-old wild-type and *LeFRK2*-antisense plants

	Wild-type	*LeFRK2*-antisense
Length (mm)	3239 ± 396^a	908 ± 251^b
Area (mm^2)	1963 ± 163^a	519 ± 123^b
Fresh weight (mg)	936 ± 95^a	331 ± 34^b
Dry weight (mg)	32 ± 3^a	15 ± 2^b
Specific length (mm/mg)	98 ± 5^a	66 ± 6^b
Specific area (mm^2/mg)	61 ± 5^a	39 ± 6^b
No. of tips per mg	7.5 ± 0.6^a	5.4 ± 0.8^b

The results are the averages and standard errors of nine root measurements for the wild-type and six for the *LeFRK2*-antisense plants. Different letters represent values that are significantly different (Student's *t* test; $P < 0.05$) between wild type and antisense plants

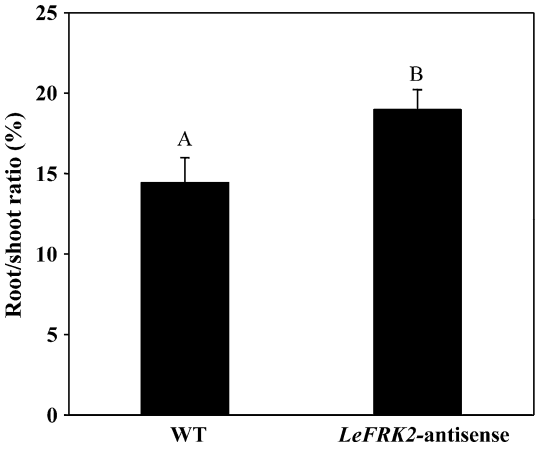

Fig. 8 Root:shoot ratio. Ratio of root dry weight to shoot dry weight. Data are the means ± SE of eight plants. *Different letters* represent values that are significantly different (student's *t* test; $P < 0.05$)

Discussion

The present study shows the key role of *LeFRK2*, the major FRK-encoding gene in tomato plants, in vascular development and function. It is the first study presenting anatomical and functional effects of specific sugar metabolism gene in vascular tissues. Suppression of *LeFRK2* substantially reduces vascular differentiation in the whole plant, resulting in narrow and short cells in both the xylem and phloem. The *LeFRK2*-antisense plants showed reduced cambium activity, vessels with thin secondary walls and small sieve elements with low levels of callose deposition. Low sucrose concentrations reduce the deposition of callose on the sieve plates in tissues grown in culture (Aloni 1980). Yet, *LeFRK2*-antisense stems had less callose despite their higher sucrose concentrations, demonstrating the importance of fructose phosphorylation by LeFRK2 for callose deposition.

The slow differentiation of secondary fibers near the cambium in the *LeFRK2*-antisense plants resulted in the formation of a region of expanding fibers, which likely squashed the fragile vessels among them, causing serious deformations in the secondary vessels. The deformed, narrow vessels reduced water conductivity in the roots, stems, and leaves. In wild-type plants, there is a gradual increase in vessel size from the young leaves to roots; so that the widest vessels are produced in roots (Aloni and Zimmermann 1983). A downward increase in vessel width was observed in our wild-type tomato plants, but was not detected in the *LeFRK2*-antisense plants, which have narrow vessels along the entire axis. Accordingly, water conductance was reduced in roots, stem, and leaves of *LeFRK2*-antisense plants; however, conductivity was most reduced in the root system (Fig. 5) and became less reduced along the water pathway from roots to leaves (Table 2 and Fig. 4).

Generally the cells in stem of *LeFRK2*-antisense plants were smaller than in the control plants. The small and short cells are probably linked to the stunted stature of *LeFRK2*-antisense plants. However, we have not found a specific change in cell structure or pattern in the parenchymatic

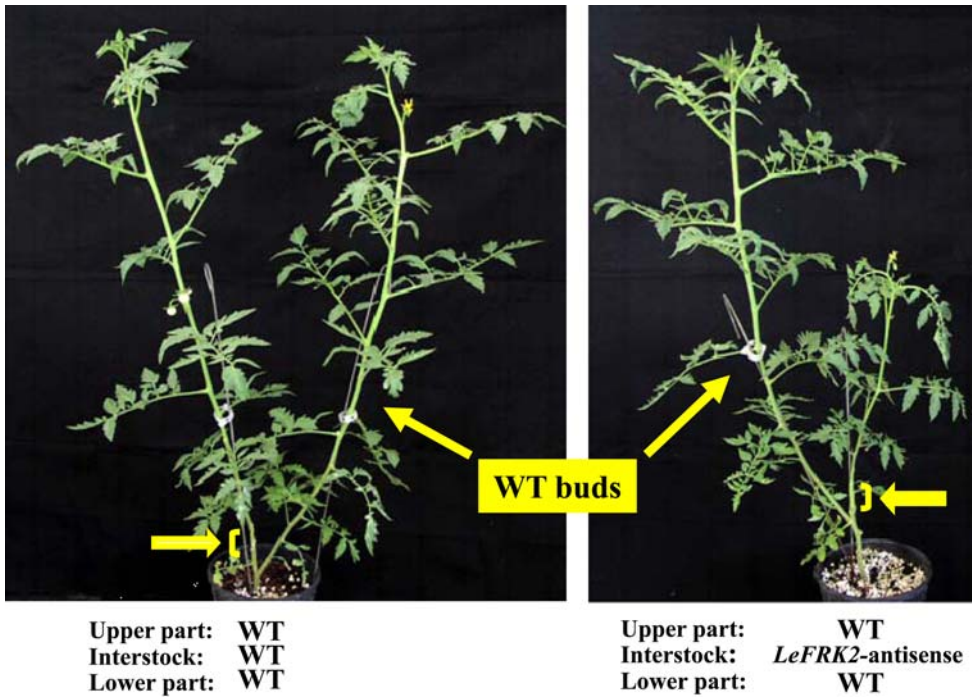

Fig. 9 Triple grafts with lateral buds. Graftings were performed in two consecutive steps (10 days apart) at the seedling stage. These plants were photographed 2 months after the second grafting. Six independent graftings of each combination were performed with similar results. The *lower*, *thicker arrows* point to the stem interstock and the *upper arrows* point to the wild-type buds that emerged from the wild-type stock

cells inside or outside the vascular tissues. It is likely therefore that *LeFRK2* is playing a specific role in differentiating vascular cells, which are probably the most actively expanding tissues in the stem.

The development of xylem and phloem is dependent on sucrose metabolism in the vascular system. To be metabolized, sucrose must be cleaved by either invertase or SuSy. SuSy has been identified in sieve elements and companion cells of tumors induced by *Agrobacterium tumefaciens* in castor beans (*Ricinus communis*) (Wachter et al. 2003). SuSy and *LeFRK2* are both expressed at high levels in the vascular tissues of tomato stems (Granot and Huber, unpublished results; German et al. 2003). SuSy cleaves sucrose into UDP-glucose and fructose; UDP-glucose may be used for cellulose and cell wall synthesis, while fructose must be phosphorylated before it can be utilized for energy production or directed into other metabolic pathways. Yet, SuSy is feedback-inhibited when its product, fructose, is present at concentrations above 1 mM (Schaffer and Petreikov 1997). Hence, the phosphorylation of fructose by *LeFRK2* might be necessary to drive sucrose cleavage, sugar metabolism, and cell wall synthesis (Pego and Smeekens 2000; German et al. 2003).

Antisense suppression of *LeFKR2* was accompanied by increasing levels of sugars in triple grafted plants with *LeFRK2*-antisense interstock (Fig. 7) as well as in intact *LeFRK2*-antisense stem (not shown). Relative water content in wild type and *LeFRK2*-antisense stem are similar (about 93%) indicating that the different sugar contents could not be attributed to different water content, but rather to reduced sugar transport and metabolism. Although glucose and sucrose are associated with developmental signals (Uggla et al. 2001), it is clear that their higher levels were insufficient to accelerate vascular development of *LeFRK2*-antisense stem.

Triple-grafting experiments indicated that *LeFRK2*-antisense interstock restricts downward phloem transport, in agreement with the anatomical observations of smaller sieve elements, yet the reduction in the specific mass transfer could not be estimated based on our anatomical data. In another study, antisense suppression of *StFRK1* (the potato homologue of *LeFRK2*) resulted in reduced tuber yield and was attributed to interrupted tuber sucrose metabolism (Davies et al. 2005), but this reduced yield may actually have been a result of reduced phloem transport. In spite of reduced phloem transport, the root:shoot ratio increased in *LeFRK2*-antisense plants, suggesting that inhibition of photoassimilate transport to roots was not the primary cause of growth inhibition. Triple grafts with lateral wild-type buds that grew from the wild-type scion further demonstrated that reduced sugar transport and inhibited root development are not the primary causes of the inhibited growth and wilting of *LeFRK2*-antisense plants. Rather, these experiments demonstrate that inhibited xylem development and reduced xylem conductivity is probably the major cause of the observed wilting and growth inhibition.

The inability of *LeFRK2*-antisense roots to develop root pressure is quite striking and could be due to interrupted xylem development and structure in roots. Alternatively, reduced sugar transport to roots of *LeFRK2*-antisense plants could also be associated with reduced expression of ion channels, as the expression of ion channels in roots is dependent on sugar metabolism (Lejay et al. 2003)

To date, four different FRK genes have been identified in tomato plants. Until recently, the major function attributed to FRKs was involvement in starch metabolism in sink tissues, largely on the basis of the concomitant activities of FRK, SuSy and starch-related genes. While FRK2 is not involved in starch metabolism (Dai et al. 2002a; Odanaka et al. 2002), it is not known whether any of the other FRKs are involved. The different expression patterns and biochemical characteristics of the different FRK genes suggest that each of these genes has a specific role. Only complete suppression of FRK2 uncovered the role of FRK2 in xylem development (German et al. 2003). Perhaps studies of the other FRK-encoding genes in transgenic plants should rely on high expression or complete suppression of these genes, an approach that has been adopted in current studies.

Acknowledgments This research was supported by research grant No. 890/06 from The Israel Science Foundation, research grants No. IS-3397-06 and No. CA-9100-06 from BARD, the United States—Israel Binational Agricultural and Development Fund. We would like to thank Dr. Yelena Yeselson for her excellent help with HPLC analyses.

References

Aloni R (1980) Role of auxin and sucrose in the differentiation of sieve and tracheary elements in plant tissue cultures. Planta 150:255–263

Aloni R, Peterson CA (1990) The functional-significance of phloem anastomoses in stems of Dahlia-Pinnata Cav. Planta 182:583–590

Aloni R, Zimmermann MH (1983) The control of vessel size and density along the plant axis—a new hypothesis. Differentiation 24:203–208

Dai N, German MA, Matsevitz T, Hanael R, Swartzberg D, Yeselson Y, Petreikov M, Schaffer AA, Granot D (2002a) *LeFRK2*, the gene encoding the major fructokinase in tomato fruits, is not required for starch biosynthesis in developing fruits. Plant Sci 162:423–430

Dai N, Kandel M, Petreikov M, Levine I, Ricard B, Rothan C, Schaffer AA, Granot D (2002b) The tomato hexokinase *LeHXK1*: cloning, mapping, expression pattern and phylogenetic relationships. Plant Sci 163:581–590

Davies HV, Shepherd LV, Burrell MM, Carrari F, Urbanczyk-Wochniak E, Leisse A, Hancock RD, Taylor M, Viola R, Ross H, McRae D, Willmitzer L, Fernie AR (2005) Modulation of fructokinase activity of potato (*Solanum tuberosum*) results in substantial shifts in tuber metabolism. Plant Cell Physiol 46:1103–1115

Dinar M, Rudich J, Zamski E (1983) Effects of heat-stress on carbon transport from tomato leaves. Ann Bot 51:97–103

German MA, Burdman S, Okon Y, Kigel J (2000) Effects of *Azospirillum brasilense* on root morphology of common bean (*Phaseolus vulgaris* L.) under different water regimes. Biol Fertil Soil 32:259–264

German MA, Dai N, Chmelnitsky I, Sobolev I, Salts Y, Barg R, Schaffer AA, Granot D (2002) *LeFRK4*, a novel tomato (*Lycopersicon esculentum* Mill.) fructokinase specifically expressed in stamens. Plant Sci 163:607–613

German MA, Dai N, Matsevitz T, Hanael R, Petreikov M, Bernstein N, Ioffe M, Shahak Y, Schaffer AA, Granot D (2003) Suppression of fructokinase encoded by LeFRK2 in tomato stem inhibits growth and causes wilting of young leaves. Plant J 34:837–846

German MA, Asher I, Petreikov M, Dai N, Schaffer AA, Granot D (2004) Cloning, expression and characterization of *LeFRK3*, the fourth tomato (*Lycopersicon esculentum* Mill.) gene encoding fructokinase. Plant Sci 166:285–291

Gorska A, Ye Q, Holbrook NM, Zwieniecki MA (2008) Nitrate control of root hydraulic properties in plants: translating local information to whole plant response. Plant Physiol 148:1159–1167

Granot D (2007) Role of tomato hexose kinases. Funct Plant Biol 34:564–570

Kanayama Y, Dai N, Granot D, Petreikov M, Schaffer A, Bennett AB (1997) Divergent fructokinase genes are differentially expressed in tomato. Plant Physiol 113:1379–1384

Kanayama Y, Granot D, Dai N, Petreikov M, Schaffer A, Powell A, Bennett AB (1998) Tomato fructokinases exhibit differential expression and substrate regulation. Plant Physiol 117:85–90

Kocacinar F, Sage RF (2004) Photosynthetic pathway alters hydraulic structure and function in woody plants. Oecologia 139:214–223

Koch K (2004) Sucrose metabolism: regulatory mechanisms and pivotal roles in sugar sensing and plant development. Curr Opin Plant Biol 7:235–246

Lejay L, Gansel X, Cerezo M, Tillard P, Muller C, Krapp A, von Wiren N, Daniel-Vedele F, Gojon A (2003) Regulation of root ion transporters by photosynthesis: functional importance and relation with hexokinase. Plant Cell 15:2218–2232

Odanaka S, Bennett AB, Kanayama Y (2002) Distinct physiological roles of fructokinase isozymes revealed by gene-specific suppression of frk1 and frk2 expression in tomato. Plant Physiol 129:1119–1126

Pego JV, Smeekens SC (2000) Plant fructokinases: a sweet family get-together. Trends Plant Sci 5:531–536

Renz A, Stitt M (1993) Substrate-specificity and product Inhibition of different forms of fructokinases and hexokinases in developing potato-tubers. Planta 190:166–175

Schaffer AA, Petreikov M (1997) Inhibition of fructokinase and sucrose synthase by cytosolic levels of fructose in young tomato fruit undergoing transient starch synthesis. Physiol Plant 101:800–806

Sinclair TR, Zwieniecki MA, Holbrook NM (2008) Low leaf hydraulic conductance associated with drought tolerance in soybean. Physiol Plant 132:446–451

Uggla C, Magel E, Moritz T, Sundberg B (2001) Function and dynamics of auxin and carbohydrates during earlywood/latewood transition in scots pine. Plant Physiol 125:2029–2039

Wachter R, Langhans M, Aloni R, Gotz S, Weilmunster A, Koops A, Temguia L, Mistrik I, Pavlovkin J, Rascher U, Schwalm K, Koch KE, Ullrich CI (2003) Vascularization, high-volume solution flow, and localized roles for enzymes of sucrose metabolism during tumorigenesis by *Agrobacterium tumefaciens*. Plant Physiol 133:1024–1037

Zwieniecki MA, Brodribb TJ, Holbrook NM (2007) Hydraulic design of leaves: insights from rehydration kinetics. Plant Cell Environ 30:910–921